Available online at www.sciencedirect.com

SCIENCE DIRECT

Biochimica et Biophysica Acta 1714 (2005) 43 – 55

BIOCHIMICA ET BIOPHYSICA ACTA BBA

http://www.elsevier.com/locate/bba

Monitoring the organization and dynamics of bovine hippocampal membranes utilizing Laurdan generalized polarization

Soumi Mukherjee, Amitabha Chattopadhyay*

Centre for Cellular and Molecular Biology, Uppal Road, Hyderabad 500 007, India

Received 30 March 2005; received in revised form 23 June 2005; accepted 23 June 2005

Abstract

Organization and dynamics of cellular membranes in the nervous system are crucial for the function of neuronal membrane receptors. The lipid composition of neuronal cells is unique and has been correlated with the increased complexity in the organization of the nervous system during evolution. Previous work from our laboratory has established bovine hippocampal membranes as a convenient natural source for studying neuronal receptors such as the G-protein coupled serotonin$_{1A}$ receptor. In this paper, we have explored the organization and dynamics of bovine hippocampal membranes using the amphiphilic environment-sensitive fluorescent probe Laurdan. Our results show that the emission spectra of Laurdan display an additional red shifted peak as a function of increasing temperature in native as well as cholesterol-depleted membranes and liposomes made from lipid extracts of the native membrane. Interestingly, wavelength dependence of Laurdan generalized polarization (GP) in native membranes indicates the presence of an ordered gel-like phase at low temperatures, whereas characteristics of the liquid-ordered phase are observed at high temperatures. Similar experiments performed using cholesterol-depleted membranes show fluidization of the membrane with increasing cholesterol depletion. In addition, results from fluorescence polarization of DPH indicate that the hippocampal membrane is fairly ordered even at physiological temperature. The temperature dependence of Laurdan excitation GP provides a measure of the apparent thermal transition temperature and extent of cooperativity in these membranes. Analysis of time-resolved fluorescence measurements of Laurdan shows reduction in mean fluorescence lifetime with increasing temperature due to change in environmental polarity. These results constitute novel information on the dynamics of hippocampal membranes and its modulation by cholesterol depletion monitored using Laurdan fluorescence.

Keywords: Bovine hippocampal membrane; Cholesterol; Laurdan generalized polarization; Temperature

1. Introduction

The lipid composition of cells that make up the nervous system is unique and has been correlated with increased complexity in the organization of the nervous system during evolution [1]. Organization and dynamics of cellular membranes in the nervous system play a crucial role in the function of neuronal membrane receptors. Cholesterol represents an important lipid in this context since it is known to regulate the function of neuronal receptors [2,3] thereby affecting neurotransmission and giving rise to mood and anxiety disorders [4]. Interestingly, the central nervous system which accounts for only 2% of the body mass contains ~25% of free cholesterol present in the whole body [5]. Although the brain is highly enriched in cholesterol, the organization and dynamics of brain cholesterol is still poorly understood [6]. Brain cholesterol is synthesized in situ [7] and is developmentally regulated [8]. Cholesterol organization, traffic, and dynamics in the brain are stringently controlled since the input of cholesterol into the central nervous system is almost exclusively from in situ synthesis as there is no evidence for the transfer of cholesterol from blood plasma to brain [5]. As a result, a number of neu-

Abbreviations: Laurdan, 6-dodecanoyl-2-(*N,N*-dimethylamino)naphthalene; BCA, bicinchoninic acid; DPH, 1,6-diphenyl-1,3,5-hexatriene; MβCD, methyl-β-cyclodextrin; DMPC, 1,2-dimyristoyl-*sn*-glycero-3-phosphocholine; PMSF, phenylmethylsulfonyl fluoride

* Corresponding author. Tel.: +91 40 2719 2578; fax: +91 40 2716 0311.
E-mail address: amit@ccmb.res.in (A. Chattopadhyay).

0005-2736/$ - see front matter © 2005 Elsevier B.V. All rights reserved.
doi:10.1016/j.bbamem.2005.06.010

rological diseases share a common etiology of defective cholesterol metabolism in the brain [9]. In the Smith–Lemli–Opitz syndrome, for example, the marked abnormalities in brain development and function leading to serious neurological and mental dysfunctions have their origin in the fact that the major input of brain cholesterol comes from in situ synthesis and such synthesis is defective in this syndrome [10]. The interaction between cholesterol and other molecular components in neuronal membranes (such as receptors and lipids) therefore assumes relevance for understanding brain function. The organization and dynamics of cellular membranes in the nervous system is thus significant for a comprehensive understanding of the functional roles played by the membrane-bound neuronal receptors which are key components in signal transduction in the nervous system.

Previous work from our laboratory has established native membranes prepared from the bovine hippocampus as a convenient natural source for studying the serotonin$_{1A}$ (5-HT$_{1A}$) receptor which is an important member of the seven transmembrane domain G-protein coupled receptor family [11]. We have partially purified and solubilized the 5-HT$_{1A}$ receptor from bovine hippocampus in a functionally active form [12]. Interestingly, the requirement of membrane cholesterol in modulating ligand binding activity of the 5-HT$_{1A}$ receptor from the bovine hippocampus has recently been shown by us [3,13–15]. In this work, we have monitored the organization and dynamics of bovine hippocampal membranes using the amphiphilic fluorescent probe Laurdan.

Laurdan is known to be very sensitive to the phase state of the membrane [16–18]. The basis of Laurdan spectral sensitivity lies in its ability to sense the polarity and dynamics of dipoles in the immediate environment due to its dipolar relaxation processes. The environment-sensitive spectroscopic properties of Laurdan have been comprehensively described by a parameter termed generalized polarization (GP), originally introduced by Gratton and coworkers [16,17]. Characteristic GP values in the pure gel (ordered) and in the pure fluid (disordered) membranes have previously been determined [19,20]. In this paper, we have utilized Laurdan fluorescence to monitor phase properties of bovine hippocampal membranes and their modulation with cholesterol and protein content.

2. Materials and methods

2.1. Materials

Cholesterol, MβCD, DMPC, DPH, EDTA, EGTA, iodoacetamide, PMSF, sucrose, polyethylenimine, sodium azide, Na_2HPO_4, Tris, and MOPS were obtained from Sigma Chemical Co. (St. Louis, MO). BCA reagent kit for protein estimation was from Pierce (Rockford, IL). Amplex Red cholesterol assay kit and Laurdan were from Molecular Probes (Eugene, OR). Concentrations of stock solutions of Laurdan and DPH in methanol were estimated from their molar extinction coefficients (ε) of 20,000 M^{-1} cm^{-1} at 364 nm, and 88,000 M^{-1} cm^{-1} at 350 nm, respectively [21]. All other chemicals used were of the highest purity available. Solvents used were of spectroscopic grade. Water was purified through a Millipore (Bedford, MA) Milli-Q system and used throughout. Fresh bovine brains were obtained from a local slaughterhouse within 10 min of death and the hippocampal region was carefully dissected out. The hippocampi were immediately flash frozen in liquid nitrogen and stored at −70 °C till further use.

2.2. Methods

2.2.1. Preparation of native hippocampal membranes

Although the membrane lipid composition of bovine hippocampus is not known, the phospholipid composition of rat hippocampus has recently been reported [22–24]. Analysis of the phospholipid composition of the rat hippocampus shows phosphatidylethanolamine, phosphatidylcholine, and phosphatidylserine as the predominant headgroups, while the fatty acid composition shows enrichment with 16:0, 18:0, 18:1, 18:2, 20:4, and 22:6 fatty acids. In addition, plasmalogens have been reported in rat hippocampus. However, there is no reported data on the possible presence of other types of lipids (such as glycosphingolipids) in hippocampus.

Native hippocampal membranes were prepared as described previously [25]. Briefly, bovine hippocampal tissue (~100 g) was homogenized as 10% (w/v) in a polytron homogenizer in buffer A (2.5 mM Tris, 0.32 M sucrose, 5 mM EDTA, 5 mM EGTA, 0.02% sodium azide, 0.24 mM PMSF, 10 mM iodoacetamide, pH 7.4). The homogenate was centrifuged at 900 × *g* for 10 min at 4 °C. The resultant supernatant was filtered through four layers of cheesecloth and centrifuged at 50,000 × *g* for 20 min at 4 °C. The pellet obtained was suspended in 10 vol. of buffer B (50 mM Tris, 1 mM EDTA, 0.24 mM PMSF, 10 mM iodoacetamide, pH 7.4) using a hand-held Dounce homogenizer and centrifuged at 50,000 × *g* for 20 min at 4 °C. This procedure was repeated until the supernatant was clear. The final pellet (native membranes) was suspended in a minimum volume of buffer C (50 mM Tris, pH 7.4), homogenized using a hand-held Dounce homogenizer, flash frozen in liquid nitrogen, and stored at −70 °C. Protein concentration was assayed using the BCA assay kit with bovine serum albumin as standard [26]. The phospholipid content of these membranes is typically ~960 nmol/mg of total protein [27]. This corresponds to a lipid/protein ratio of ~0.75 (w/w) which is similar to lipid/protein ratio found in human erythrocytes [28].

2.2.2. Cholesterol depletion of native membranes

Native hippocampal membranes were depleted of cholesterol using MβCD as described previously [3,27].

Briefly, membranes with a total protein concentration of 2 mg/ml were treated with different concentrations of MβCD in 10 mM MOPS buffer (pH 7.4) at 25 °C in a temperature controlled water bath with constant shaking for 1 h. Membranes were then spun down at 50,000 × *g* for 5 min, washed once with MOPS buffer, and resuspended in the same buffer. Cholesterol was estimated using the Amplex Red cholesterol assay kit [29].

2.2.3. Lipid extraction from native and cholesterol-depleted membranes

Lipid extraction was carried out according to the method of Bligh and Dyer [30] from native hippocampal membranes and native membranes treated with 40 mM MβCD. The lipid extract was finally resuspended in a mixture of chloroform–methanol (1:1, v/v).

2.2.4. Estimation of inorganic phosphate

Concentration of lipid phosphate was determined subsequent to total digestion by perchloric acid [31] using Na_2HPO_4 as standard. DMPC was used as an internal standard to assess lipid digestion. Samples without perchloric acid digestion produced negligible readings.

2.2.5. Sample preparation

Membranes (native and cholesterol-depleted) containing 100 nmol of total phospholipid were suspended in 2 ml of 10 mM MOPS buffer (pH 7.4). The amount of Laurdan (or DPH) added from a methanolic stock solution was such that the final fluorophore concentration was 1 mol% with respect to the total phospholipid content. The resultant probe concentration was 0.5 μM in all cases and the methanol content was always low (0.4–0.6%, v/v). This ensures optimal fluorescence intensity with negligible membrane perturbation. The fluorophore was added to membranes while being vortexed for 1 min and kept in the dark for 1 h before measurements. Background samples were prepared the same way except that fluorophores were omitted. The protein concentration was ~0.04 mg/ml.

Lipid extracts containing 100 nmol of total phospholipid in chloroform–methanol (1:1, v/v) were mixed well with 1 nmol of Laurdan (or DPH) in methanol. The sample was mixed well and dried under a stream of nitrogen while being warmed gently (~45 °C). After further drying under a high vacuum for at least 6 h, 2 ml of 10 mM MOPS, pH 7.4 buffer was added and lipid samples were hydrated (swelled) at ~70 °C while being intermittently vortexed for 3 min to disperse the lipid and form homogeneous multilamellar vesicles (MLVs). The MLVs were kept at ~70 °C for an additional hour to ensure proper swelling as the vesicles were made. Such high temperatures were necessary for hydrating the samples due to the presence of lipids with high melting temperature in neuronal tissues [32]. Samples were kept in the dark at room temperature (25 °C) overnight before taking fluorescence measurements. MOPS buffer was used to avoid any change in pH due to temperature change since the change in pK_a/°C for MOPS is negligible (−0.006) [33].

2.2.6. Generalized polarization measurements

Steady state fluorescence measurements with Laurdan were performed with a Hitachi F-4010 steady state spectrofluorometer equipped with a stirring accessory and thermostated (±0.1 °C) by a circulating water bath, using 1 cm path length quartz cuvettes. While heating, the sample temperature was continuously measured with a thermocouple. Excitation and emission slits with nominal bandpass of 5 nm were used for all measurements. Background intensities of samples in which the fluorophore was omitted were subtracted from each sample spectrum to cancel out any contribution due to scattering artifacts. The optical density of the samples measured at 355 nm was ~0.18.

Excitation GP (GP_{ex}) was calculated according to the equation [16,17]:

$$GP_{ex} = \frac{I_{434} - I_{482}}{I_{434} + I_{482}} \quad (1)$$

where I_{434} and I_{482} are the measured fluorescence intensities (after appropriate background subtraction) at the characteristic emission wavelengths of the gel phase (434 nm) and the liquid-crystalline phase (482 nm), respectively. In the case of calculation of excitation GP (GP_{ex}), emission wavelengths of 434 and 482 nm actually correspond to the maximum emission of the gel and liquid-crystalline phases, respectively. Excitation GP (GP_{ex}) values were obtained from emission spectra at different excitation wavelengths (355–420 nm) or at only one excitation wavelength (355 nm) where indicated. GP values range from −1 (most fluid) to +1 (most ordered) membranes and are independent of concentration of Laurdan.

Emission GP (GP_{em}) was calculated according to the equation [16,17]:

$$GP_{em} = \frac{I_{410} - I_{340}}{I_{410} + I_{340}} \quad (2)$$

where I_{410} and I_{340} are the measured fluorescence intensities (after appropriate background subtraction) at the characteristic excitation wavelengths of 410 and 340 nm, respectively. In the case of calculation of emission GP (GP_{em}), excitation wavelengths of 340 and 410 nm do not correspond to the maximum excitation of the liquid-crystalline and of the gel phases, respectively. They were chosen as convenient extremes of the excitation spectrum to improve the photoselection of the two Laurdan populations [19]. Emission GP (GP_{em}) values were obtained from excitation spectra at different emission wavelengths (420–500 nm).

2.2.7. Time-resolved fluorescence measurements

Fluorescence lifetimes were calculated from time-resolved fluorescence intensity decays using a Photon Technology International (London, Western Ontario, Can-

ada) LS-100 luminescence spectrophotometer in the time-correlated single photon counting mode, thermostated (±0.1 °C) by a circulating waterbath, using 1 cm path length quartz cuvettes. While heating, the sample temperature was continuously measured with a thermocouple. This machine uses a thyratron-gated nanosecond flash lamp filled with nitrogen as the plasma gas (16±1 in. of mercury vacuum) and is run at 17–22 kHz. Lamp profiles were measured at the excitation wavelength using Ludox (colloidal silica) as the scatterer. To optimize the signal to noise ratio, 10,000 photon counts were collected in the peak channel. The excitation wavelength used was 358 nm which corresponds to a peak in the spectral output of the nitrogen lamp. Emission wavelength was set at 434 nm. All experiments were performed using excitation and emission slits with a nominal bandpass of 4 nm or less. The sample and the scatterer were alternated after every 5% acquisition (i.e., after 500 counts are collected in the peak channel each time) to ensure compensation for shape and timing drifts occurring during the period of data collection. This arrangement also prevents any prolonged exposure of the sample to the excitation beam thereby avoiding any possible photodamage of the fluorophore. The data stored in a multichannel analyzer was routinely transferred to an IBM PC for analysis. Fluorescence intensity decay curves so obtained were deconvoluted with the instrument response function and analyzed as a sum of exponential terms:

$$F(t) = \sum_i \alpha_i \exp(-t/\tau_i) \tag{3}$$

where $F(t)$ is the fluorescence intensity at time t and α_i is a preexponential factor representing the fractional contribution to the time-resolved decay of the component with a lifetime τ_i such that $\sum_i \alpha_i = 1$. The decay parameters were recovered using a nonlinear least squares iterative fitting procedure based on the Marquardt algorithm [34]. The program also includes statistical and plotting subroutine packages [35]. The goodness of the fit of a given set of observed data and the chosen function was evaluated by the reduced χ^2 ratio, the weighted residuals [36], and the autocorrelation function of the weighted residuals [37]. A fit was considered acceptable when plots of the weighted residuals and the autocorrelation function showed random deviation about zero with a minimum χ^2 value not more than 1.4. Mean (average) lifetimes $<\tau>$ for biexponential decays of fluorescence were calculated from the decay times and preexponential factors using the following equation [38]:

$$<\tau> = \frac{\alpha_1\tau_1^2 + \alpha_2\tau_2^2}{\alpha_1\tau_1 + \alpha_2\tau_2} \tag{4}$$

2.2.8. Fluorescence polarization measurements

Steady state fluorescence polarization measurements with DPH were performed with a Hitachi F-4010 steady state spectrofluorometer equipped with a stirring accessory and thermostated (±0.1 °C) by a circulating water bath, using 1 cm path length quartz cuvettes. While heating, the sample temperature was continuously measured with a thermocouple. Excitation and emission wavelengths were set at 358 and 430 nm. Excitation and emission slits with nominal bandpasses of 1.5 nm and 20 nm were used. The excitation slit was kept low to avoid any photoisomerization of DPH. In addition, fluorescence was measured with a 30-s interval between successive openings of the excitation shutter (when the sample was in the dark in the fluorimeter) to reverse any photoisomerization of DPH [39]. The optical density of the samples measured at 358 nm was 0.18±0.01. The polarization values remained identical even after dilution of membrane samples indicating the absence of any scattering artifact [40]. Fluorescence polarization measurements were performed using a Hitachi polarization accessory. Polarization values were calculated from the equation [38]:

$$P = \frac{I_{VV} - GI_{VH}}{I_{VV} + GI_{VH}} \tag{5}$$

where I_{VV} and I_{VH} are the measured fluorescence intensities (after appropriate background subtraction) with the excitation polarizer vertically oriented and the emission polarizer vertically and horizontally oriented, respectively. G is the grating correction factor and is equal to I_{HV}/I_{HH}. All experiments were done with multiple sets of samples and average values of fluorescence polarization are shown in Fig. 8.

3. Results

3.1. Laurdan fluorescence characteristics in hippocampal membranes

The normalized emission spectra of Laurdan in native hippocampal membranes as a function of increasing temperature are shown in Fig. 1a. The emission maximum was found to be 434 nm (characteristic of the gel phase) at low temperatures. This is consistent with an earlier report in which fluorescence polarization measurements showed that the native hippocampal membrane exhibits considerable rigidity [27]. The emission spectra show an additional peak at ~482 nm at high temperatures. Such a red shifted emission peak has previously been reported for phospholipids in the liquid-crystalline (fluid) phase, in which the rate of dipolar relaxation is high [17]. This suggests that at high temperatures, the membrane becomes more fluid thereby imparting higher mobility at the membrane interface (where Laurdan is localized) which leads to an increase in the dipolar relaxation in this region of the membrane. Interestingly, Laurdan emission spectra in liposomes made from lipid extract of native membranes exhibit similar temperature dependence (see Fig. 1b) as was observed with native membranes. This indicates that the polarity and dynamics of

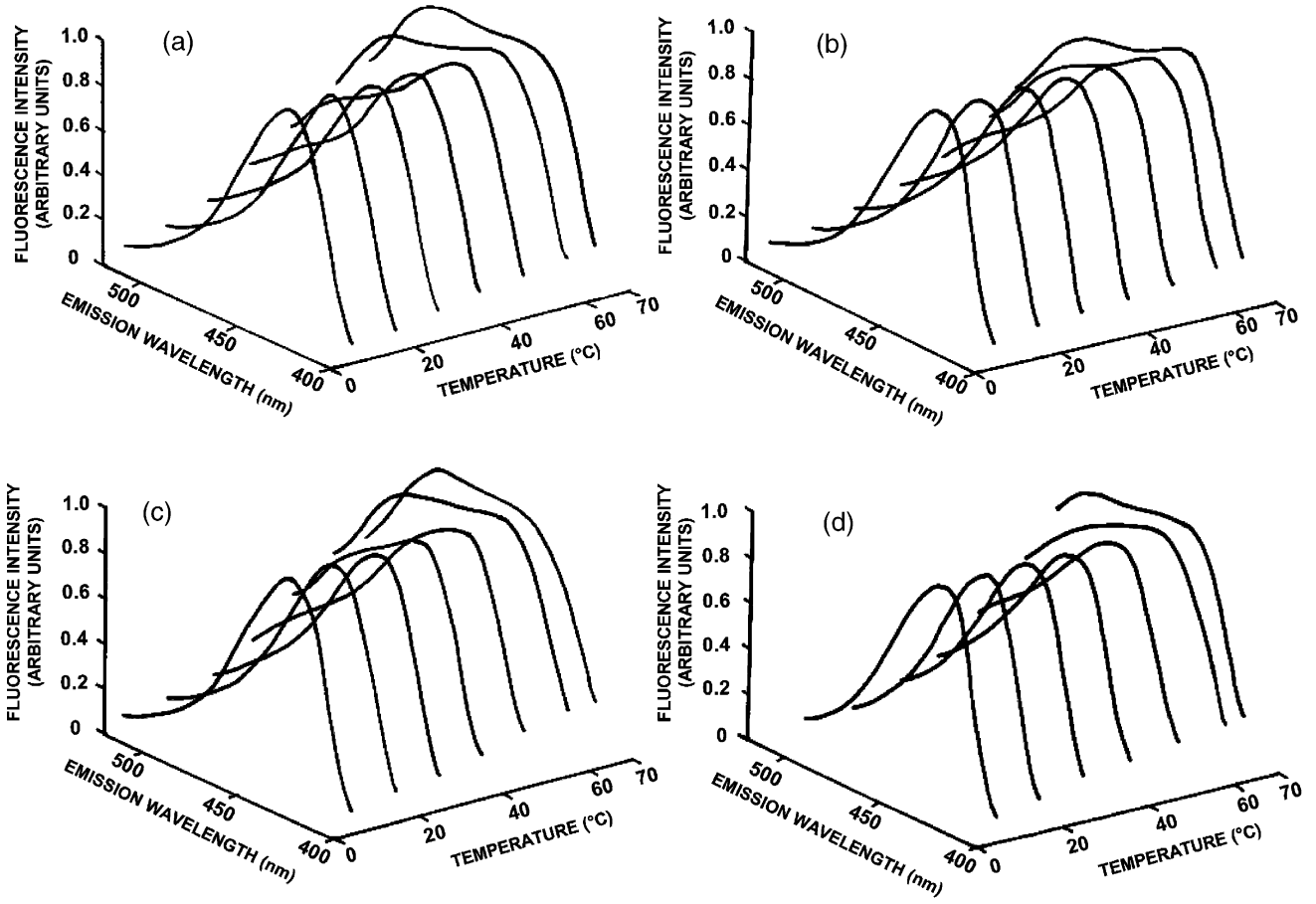

Fig. 1. Normalized emission spectra of Laurdan in (a) native bovine hippocampal membranes, (b) liposomes of lipid extract from native membranes, (c) cholesterol-depleted (with 40 mM MβCD) membranes, and (d) liposomes of lipid extract from cholesterol-depleted (with 40 mM MβCD) membranes, as a function of increasing temperature (5–62 °C). The excitation wavelength used was 355 nm. The ratio of fluorophore (Laurdan) to total phospholipid was maintained at 1:100 (mol/mol). The protein concentration is ~0.04 mg/ml. See Materials and methods for other details.

the lipids are similar in native membranes and in liposomes made from lipid extracts of native membranes which are devoid of protein but would contain a high endogenous cholesterol level.

We carried out cholesterol depletion in native hippocampal membranes using MβCD which is a water-soluble compound, and has previously been shown to selectively and efficiently extract cholesterol from membranes by including it in a central nonpolar cavity [41]. Table 1 shows that upon treatment with increasing concentrations of MβCD, the cholesterol content of bovine hippocampal membranes shows progressive reduction. Thus, when native membranes are treated with 10 mM MβCD, the cholesterol content is reduced to ~62% of the initial value. This effect levels off with increasing concentrations of MβCD, with the cholesterol content of hippocampal membranes being reduced to ~10% of the original value when the membranes are treated with 40 mM MβCD (see Table 1). Importantly, Table 1 shows that the change in phospholipid content under these conditions was found to be negligible (<9%) in all cases. This shows that the depletion of cholesterol by MβCD is specific (see also [3]). The emission spectra of Laurdan in cholesterol-depleted hippocampal membranes are shown in Fig. 1c as a function of increasing temperature. Interestingly, an increase in the ratio of intensities of the peaks at 482 and 434 nm is observed at higher temperatures. This indicates an increase in the liquid-crystalline (fluid) component of the membrane under these conditions possibly due to cholesterol depletion. These results are supported by the earlier observation that cholesterol depletion of native hippocampal membranes leads to a decrease in membrane order as monitored by fluorescence polarization [3]. In addition, Laurdan emission spectra in liposomes made from lipid extracts of cholesterol-depleted membranes display temperature dependence similar to cholesterol-depleted membranes (see Fig. 1d).

3.2. Wavelength dependence of Laurdan fluorescence properties in hippocampal membranes

Useful information about the membrane phase state could be obtained by monitoring the environment of Laurdan utilizing the wavelength dependence of its GP spectra [17,18,42–44]. Fig. 2 shows a schematic represen-

Table 1
Effect of cholesterol depletion on the apparent thermal transition temperature and cooperativity of transition in lipid extracts and natural membranes[a]

Membrane condition	Chol/PL (mol/mol)	Chol[b] (mol%)	PL[c] (mol%)	T_m (°C)	p (°C)
Native	0.45	100	100	52.5±5.7	−0.0251
Lipid extract	ND[d]	ND[d]	ND[d]	63.9±7.8	−0.0214
Cholesterol-depleted membranes treated with					
(i) 10 mM MβCD	0.34	62.2	97.1	49.1±2.9	−0.0325
(ii) 20 mM MβCD	0.19	29.1	97.1	43.3±0.8	−0.0359
(iii) 30 mM MβCD	0.13	18.0	94.3	–	–
(iv) 40 mM MβCD	0.07	9.8	91.4	43.2±0.8	−0.0368
Lipid extract from cholesterol-depleted membranes treated with 40 mM MβCD	ND[d]	ND[d]	ND[d]	48.1±0.1	−0.0412

[a] The apparent thermal transition temperature (T_m) and the slope factor (p) were determined as described in Fig. 7. The data shown for T_m represent the mean±standard error derived from the nonlinear curve fitting. See Fig. 7 for other details.
[b] Values are expressed as percentages of cholesterol content in native membranes without MβCD treatment.
[c] Values are expressed as percentages of phospholipid content in native membranes without MβCD treatment.
[d] Not determined.

tation of the wavelength dependence of Laurdan excitation and emission GP spectra in different phase states of the membrane. A wavelength independent GP spectrum is characteristic of the gel phase. In liquid-crystalline phases, on the other hand, the GP spectrum typically displays wavelength dependence, due to the dipolar relaxation process. The basis of this effect lies in the change in fluorophore-solvent interactions in the ground and excited states, brought about by a change in the dipole moment of the fluorophore upon excitation, and the rate at which solvent molecules reorient around the excited state dipole [45]. The change in the dipole moment upon excitation causes the solvent dipoles to reorient in response to this altered dipole moment to attain an energetically favorable orientation. This rate of solvent reorientation depends on the phase state of the membrane (i.e., gel or liquid-crystalline phase). Laurdan fluorescence is sensitive to the polarity of its environment and its dipole moment changes ~5–8 Debye upon excitation [46,47]. The origin of the dipolar relaxation process is thought to be due to the presence of a few water dipoles at the membrane interface, a region where the fluorescent naphthalene moiety of Laurdan is localized [19]. The relaxation (reorientation) time of these water molecules is of the same order of magnitude as the fluorescence lifetime of Laurdan when the membrane is in the liquid-crystalline state, i.e., the excited state dipole of Laurdan can align neighboring solvent dipoles with molecular dynamics in the same order of magnitude as the fluorescence lifetime of Laurdan [48]. In the liquid-crystalline state, the excitation GP values decrease with increasing excitation wavelength while the emission GP values show an increase with increasing emission wavelength. In the case of two coexisting phases, the GP spectrum shows the opposite trend (i.e., the excitation GP values increase with excitation wavelength and the emission GP values show a reduction with emission wavelength) due to the photoselection process. Interestingly, when two phases coexist, high cholesterol concentrations (>30 mol%) reverse the above trend of the GP spectral dependence, such that no more photoselection occurs and a spectral behavior similar to that of the liquid-crystalline phase (but with higher GP values) is exhibited. This type of dependence implies the presence of a single liquid-ordered phase characterized by fast dipolar relaxation with high GP values [19,49]. This phase has properties typical of the liquid-crystalline (fast lateral diffusion) and the gel (or ordered) phase characterized by ordered acyl chains resulting from the dual effect of cholesterol (i.e., rigidifying fluid membranes and fluidizing gel membranes).

The wavelength dependence of Laurdan GP for the native hippocampal membranes as a function of increasing temperature (5–62 °C) is shown in Figs. 3a and b. Excitation and emission GP values were calculated using Eqs. (1) and (2). The spectra show decreasing values of excitation GP with increasing excitation wavelength (360–410 nm) while that of emission GP show an increase with increasing emission wavelength (420–500 nm). The excitation GP spectra at relatively low temperatures (up to 15 °C) display high GP values and do not show considerable wavelength dependence although a slight dependence at wavelengths >385 nm is observed (see Fig. 3a). This implies the predominance of ordered gel-like membranes at low temperatures. At higher temperatures, both excitation and emission GP display considerable wavelength dependence typical of fluid phase while exhibiting high GP values. This indicates the presence of dipolar relaxation and lack of photoselection. These two characteristics indicate that the environment of Laurdan in native membranes at high temperatures resembles the liquid-ordered phase. This could possibly be attributed to high levels (~31 mol%) of

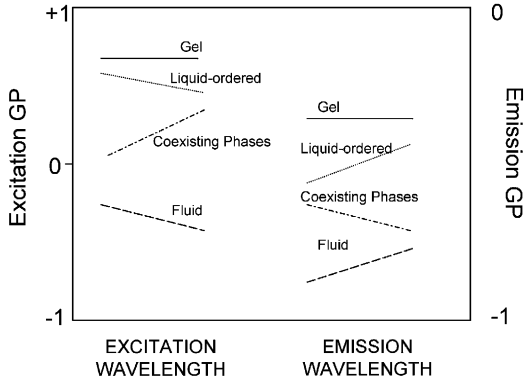

Fig. 2. A schematic representation of the wavelength dependence of Laurdan excitation and emission GP spectra of the gel (–), liquid-ordered (····), fluid (–), and coexisting gel and fluid (-·-) phospholipid phases (adapted and modified from Refs. [18,20,44]).

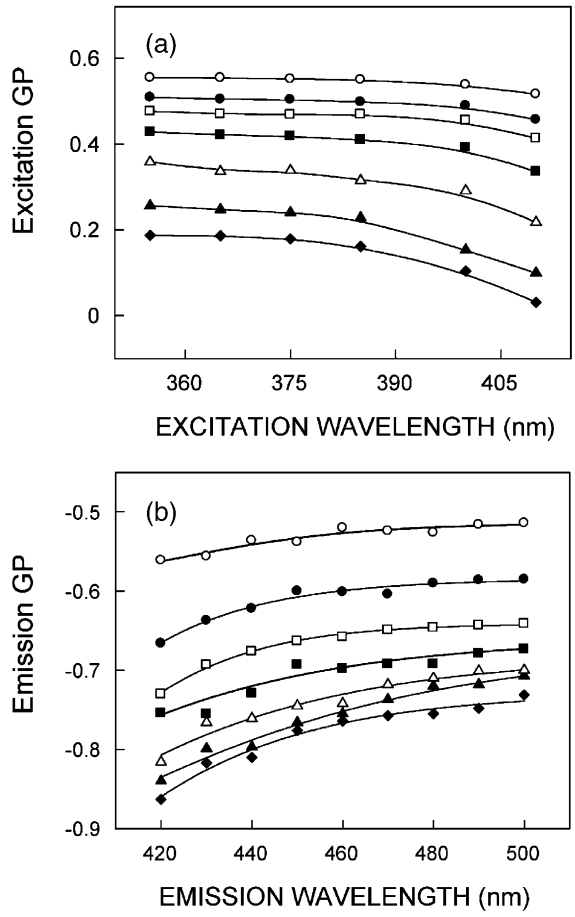

Fig. 3. Wavelength dependence of Laurdan GP in native bovine hippocampal membranes as a function of increasing temperature. Panel (a) shows the effect of changing excitation wavelength on excitation GP while panel (b) shows the effect of changing emission wavelength on emission GP at 5 °C (○), 15 °C (●), 25 °C (□), 35 °C (■), 45 °C (△), 55 °C (▲) and 62 °C (♦). Data shown are the means ± standard error of multiple measurements. Standard errors are <0.05 and are not shown for the sake of clarity. All other conditions are as in Fig. 1. See Materials and methods for other details.

cholesterol (see Table 1) in native hippocampal membranes, since liquid-ordered phase membranes typically contain high amounts of cholesterol [50].

Fig. 4 shows the wavelength dependence of Laurdan GP for native hippocampal membranes as a function of increasing temperature (5–62 °C) and cholesterol depletion. The spectra in all cases show decreasing values of excitation GP with increasing excitation wavelength (360–420 nm, Figs. 4a–c) while emission GP show an increase with increasing emission wavelength (420–500 nm, Figs. 4d–f). Specifically, the excitation GP show lower values, especially at higher temperatures and higher concentrations of MβCD used, indicating that cholesterol depletion causes more fluidization of the membrane and this trend increases as the extent of cholesterol depletion is increased by increasing concentrations of MβCD. To make this point clear, we have plotted the effect of increasing concentrations of MβCD (Fig. 5a) and the accompanying reduction in cholesterol content (Fig. 5b) for hippocampal membranes on Laurdan excitation GP at representative temperatures (5, 35 and 62 °C). Excitation GP values corresponding to excitation at 355 and 410 nm were chosen for this plot in order to appreciate the dipolar relaxation process which involves photoselection of molecules with different extents of relaxation. Excitation at red edge (410 nm) photoselects a subclass of Laurdan molecules which are 'solvent-relaxed' due to strong interaction with the solvent molecules in the excited state. It is clear from the figure that the decrease in excitation GP is more pronounced at high temperature when excited at longer wavelength (410 nm). In addition, this effect is enhanced with increasing cholesterol depletion.

The wavelength dependence of Laurdan GP in liposomes prepared from lipid extracts from native membranes as a function of increasing temperature is shown in Fig. 6. The overall trend in this case also remains similar, i.e., decreasing values of excitation GP with increasing excitation wavelength (Fig. 6a) while that of emission GP show an increase with increasing emission wavelength (Fig. 6b). Interestingly, the excitation GP values are somewhat lower at higher temperatures suggesting fluidization of the membrane due to the removal of proteins which could have tightly bound lipid molecules associated with them.

3.3. Temperature dependence of Laurdan excitation GP and fluorescence lifetime in hippocampal membranes

In order to study the thermotropic properties of hippocampal membranes, we monitored the temperature dependence of excitation GP values with increasing extents of cholesterol depletion (Fig. 7). Since natural membranes do not exhibit distinct phase transitions [42,51], these plots do not exhibit sharp phase transitions. However, there is a gradual change of membrane order as a function of temperature. Nonetheless, we fitted the data of change in excitation GP with temperature to a sigmoidal regression function to derive a value for the 'apparent' thermal transition temperature (T_m) and the slope factor (p) [20,52] which provide a measure of the extent of cooperativity of the transition (see Fig. 7 and Table 1). Table 1 shows that with progressive cholesterol depletion, the apparent thermal transition temperature decreases. This decrease is most pronounced up to 20 mM MβCD used after which it levels off. This is accompanied by an increase in the slope factor implying that the cooperativity index increases upon cholesterol depletion. Taken together, this suggests that cholesterol depletion results in a relatively homogeneous membrane. Surprisingly, liposomes made from lipid extract from the native membrane show an increase in apparent thermal transition temperature with a concomitant reduction of the cooperative index. This indicates that the packing of lipid molecules is tighter in absence of proteins and the possibility of the presence of higher melting long chain lipids in the membrane. In fact,

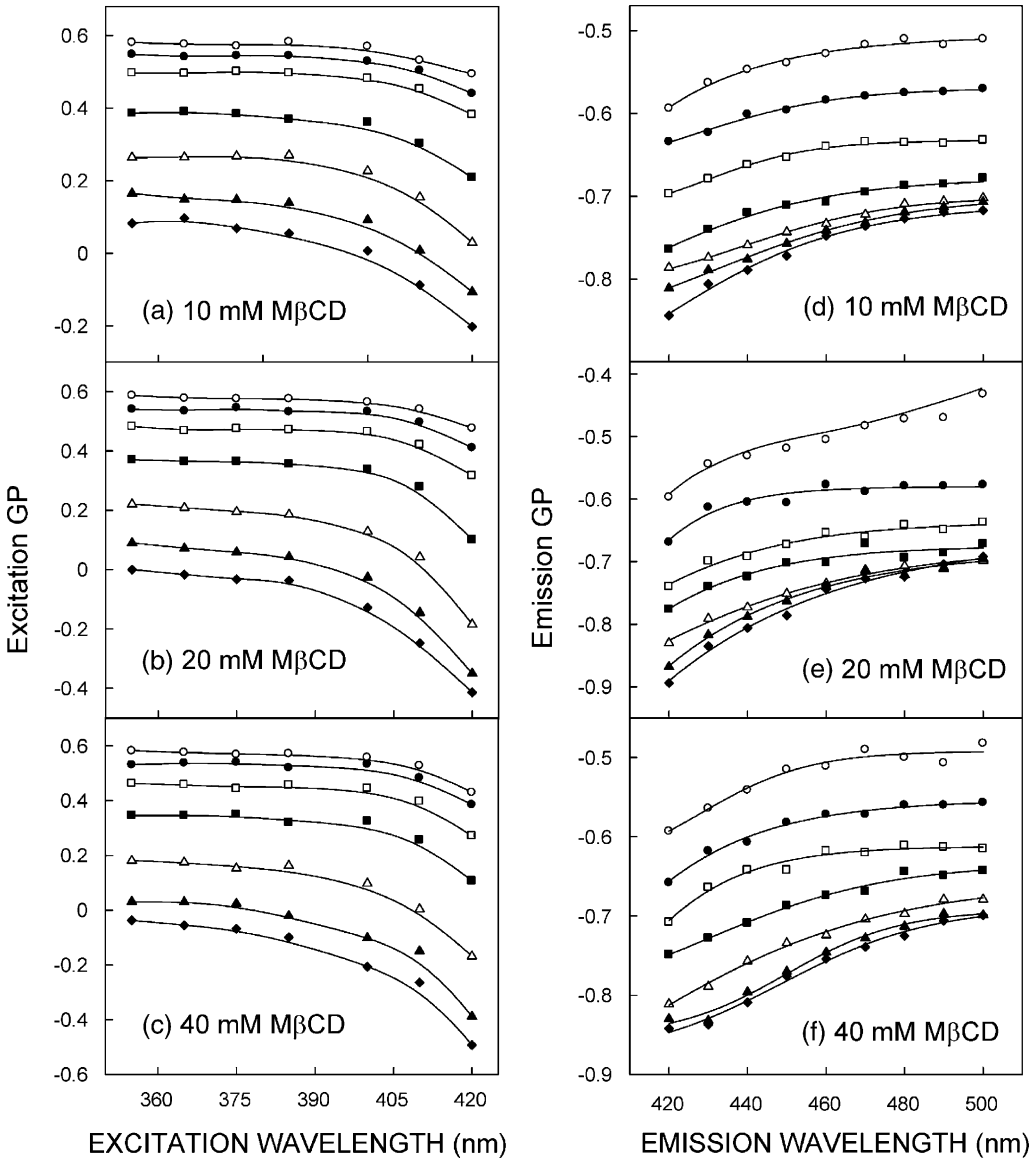

Fig. 4. Wavelength dependence of Laurdan GP in native membranes treated with increasing concentrations of MβCD as a function of increasing temperature: 5 °C (○), 15 °C (●), 25 °C (□), 35 °C (■), 45 °C (△), 55 °C (▲), and 62 °C (♦). Panels (a)–(c) show the effect of changing excitation wavelength on excitation GP with increasing concentrations of MβCD (10–40 mM). Panels (d)–(f) show the corresponding effect of changing emission wavelength on emission GP with increasing concentrations of MβCD. All other conditions are as in Fig. 3. See Materials and methods for other details.

such lipids have been shown to be present in rat hippocampus [22–24]. Interestingly, lipid extracts from the cholesterol-depleted membrane using 40 mM MβCD (see inset of Fig. 7) show an increase in transition temperature (from 43.2 to 48.1 °C) with an increase in cooperative index.

Fluorescence lifetime serves as a sensitive indicator of the local environment in which a given fluorophore is placed [53]. In addition, it is well known that the fluorescence lifetime of Laurdan is sensitive to the environment in which it is placed. The fluorescence lifetime of Laurdan has previously been reported to be ~6 ns in the gel phase and ~3 ns in the liquid-crystalline (fluid) phase [44]. The observed reduction in fluorescence lifetime could be attributed to an increase in polarity of the microenvironment which increases the rate of nonradiative decay. The effect of temperature on fluorescence lifetime of Laurdan incorporated into native and cholesterol-depleted hippocampal membranes and in liposomes made from lipid extracts from native membranes is shown in Table 2. As seen from the table, all fluorescence decays could be fitted well with a biexponential function. We chose to use the mean fluorescence lifetime as an important parameter for describing the behavior of Laurdan in these membranes since it is independent of the number of exponentials used to fit the time-resolved fluorescence decay. The mean fluorescence lifetimes were calculated using Eq. (4) and shown in Table 2. The mean fluorescence lifetime of Laurdan decreases in all cases with increasing temperature due to increased water penetration in the membrane [54]. The fluorescence lifetime

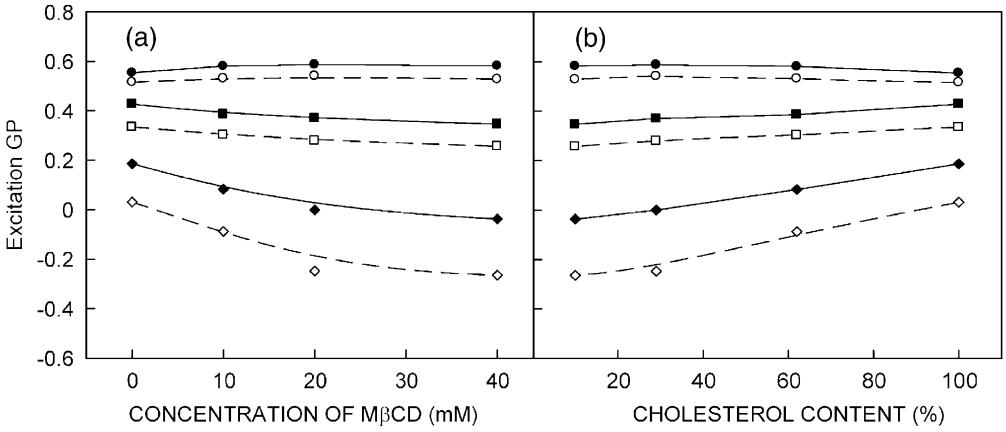

Fig. 5. Effect of (a) increasing concentrations of MβCD and (b) accompanying cholesterol depletion (as shown in Table 1) in bovine hippocampal membranes on Laurdan excitation GP at different temperatures and when excited at 355 (solid lines) and 410 nm (dashed lines). The temperatures correspond to 5 °C (● and ○), 35 °C (■ and □) and 62 °C (♦ and ◇). All other conditions are as in Fig. 3. See Materials and methods for other details.

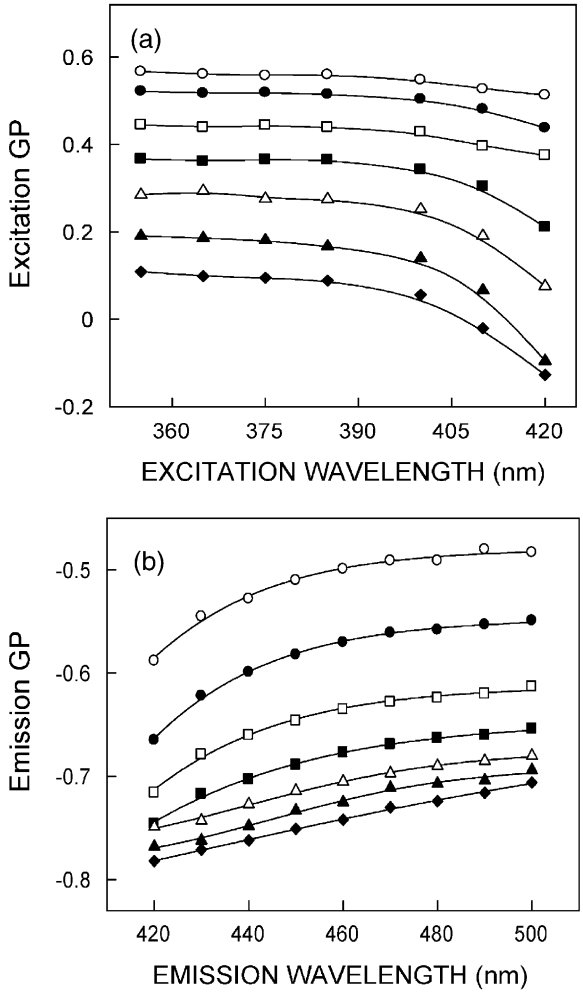

Fig. 6. Wavelength dependence of Laurdan GP in liposomes prepared from lipids extract from native membranes as a function of increasing temperature. Panel (a) shows the effect of changing excitation wavelength on excitation GP while panel (b) shows the effect of changing emission wavelength on emission GP at 5 °C (○), 15 °C (●), 25 °C (□), 35 °C (■), 45 °C (△), 55 °C (▲), and 62 °C (♦). All other conditions are as in Fig. 3. See Materials and methods for other details.

values of Laurdan in native and cholesterol-depleted membranes at low temperatures reinforce our earlier results that the native and cholesterol-depleted membranes display considerable rigidity (order) (see also Fig. 4). The mean fluorescence lifetime of Laurdan shows considerable reduction in liposomes from lipid extracts, although the effect of temperature is much less pronounced. Interestingly, while the extent of reduction in mean fluorescence lifetime for native and cholesterol-depleted membranes as a function of increasing temperature are similar (~50%), it is considerably less in case of lipid extracts (~18%). This could indicate relatively loose packing of the membrane components in the presence of bulky proteins allowing more water penetration which reduces Laurdan lifetime. The packing in lipid extracts is tighter resulting in less water penetration and therefore giving rise to lesser extent in the change in lifetime.

3.4. Temperature dependence of fluorescence polarization of DPH in hippocampal membranes

In order to monitor any change in the overall order of hippocampal membranes, we measured the steady state fluorescence polarization of the well characterized membrane probe DPH. DPH and its derivatives represent popular membrane probes for monitoring organization and dynamics in membranes [55]. Fluorescence polarization is correlated to the rotational diffusion of membrane embedded probes which is sensitive to the packing of fatty acyl chains and cholesterol [38]. The fluorescence polarization of DPH does not show any trend with temperature for native hippocampal membranes and cholesterol-depleted membranes (see inset of Fig. 8), possibly due to the presence of proteins [28]. However, liposomes made from lipid extract from the native membrane show a characteristic decrease in polarization with increasing temperature (see Fig. 8). Interestingly, the polarization remains high even at high temperatures indicating that the overall order of the membrane is maintained

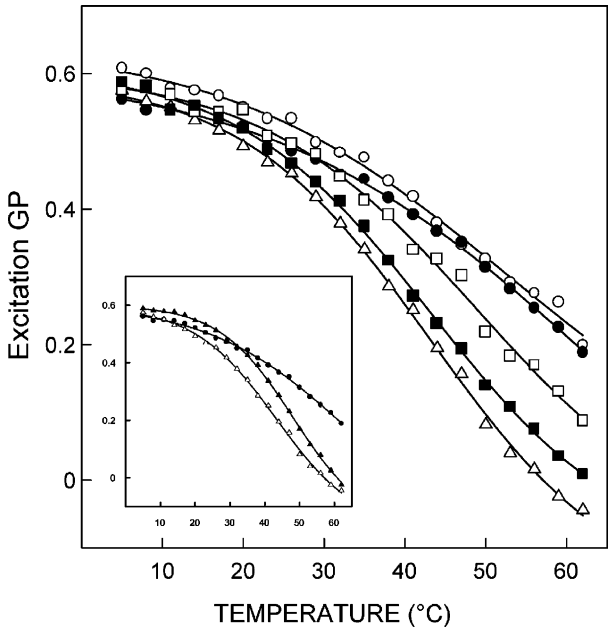

Fig. 7. Excitation GP of Laurdan in native membranes (○), and in native membranes treated with 10 mM (□), 20 mM (■), 40 mM MβCD (△), and in liposomes prepared from lipid extract from native membranes (●) as a function of temperature. The inset shows excitation GP of Laurdan in liposomes prepared from lipid extract from native membranes treated with 40 mM MβCD (▲) as a function of temperature. For comparison, data for native membranes treated with 40 mM MβCD (△) and lipid extract from native membranes (●) are also shown in the inset. Excitation wavelength used was 355 nm and emission was monitored at 434 and 482 nm. The data were fitted to a sigmoidal regression function (solid lines) to derive a value for the midpoint temperature (T_m) for a 50% change in the excitation GP values as a function of increasing temperature. The equation used was $GP(T)=GP_1+[(GP_2-GP_1)/(1+10^{p(T_m-T)})]$, where GP($T$) was the measured excitation GP at a given temperature (T), GP_1 and GP_2 are the bottom and top asymptote values of GP, T_m is the apparent thermal transition temperature of the membrane (and corresponds to a 50% change in the excitation GP values as a function of increasing temperature), and p is the slope factor which refers to the Hill Slope (describes the steepness of the curve). The slope factor provides a measure of the extent of cooperativity during membrane phase transition, and is negative since the curve goes downhill. The values of the apparent thermal transition temperature (T_m) and the slope factor (p) under various conditions are shown in Table 1. All other conditions are as in Fig. 3. See Materials and methods for other details.

even at high temperatures. The change in polarization with increase in temperature is almost linear in case of liposomes from lipid extract from cholesterol-depleted membranes with an overall lowering of polarization.

4. Discussion

In this paper, we have explored the organization and dynamics of bovine hippocampal membranes using Laurdan fluorescence. Knowledge of dynamics would help in analyzing functional data generated by modulation of membrane lipid composition [3]. Use of Laurdan fluorescence in analyzing dynamics of natural membranes is advantageous since generalized polarization is not affected

Table 2
Effect of temperature on mean fluorescence lifetime of Laurdan[a]

Temperature (°C)	α_1	τ_1 (ns)	α_2	τ_2 (ns)	$<\tau>$ (ns)[b]
Native membranes					
20	0.45	6.96	0.55	3.76	5.69
30	0.29	6.54	0.71	3.53	4.83
40	0.29	5.32	0.71	2.83	3.91
50	0.17	4.39	0.83	2.31	2.89
Cholesterol-depleted membranes by treatment with 40 mM MβCD					
20	0.28	8.40	0.72	3.36	5.84
30	0.20	7.83	0.80	2.82	4.87
40	0.14	7.14	0.86	2.43	3.95
50	0.06	6.46	0.94	2.16	2.85
Lipid extract from native membranes					
20	0.08	8.72	0.92	2.33	3.90
30	0.08	8.29	0.92	2.24	3.71
40	0.07	8.12	0.93	1.95	3.42
50	0.06	7.96	0.94	1.90	3.18

[a] Excitation wavelength was 358 nm and emission was monitored at 434 nm. All other conditions are as in Fig. 3. See Materials and Methods for other details.
[b] Calculated using Eq. (4).

by scattering artifacts [56]. In addition, GP measurements provide dynamic information on the phase state of the membrane from steady state measurements even without the use of polarizers. Laurdan has been shown to be localized at the membrane interface [57] using the parallax method [58]. Laurdan is very weakly fluorescent in water, and upon transfer to a hydrophobic medium, fluoresces brightly in the visible range and exhibits a high degree of environmental sensitivity [56] due to the presence of the 12-carbon

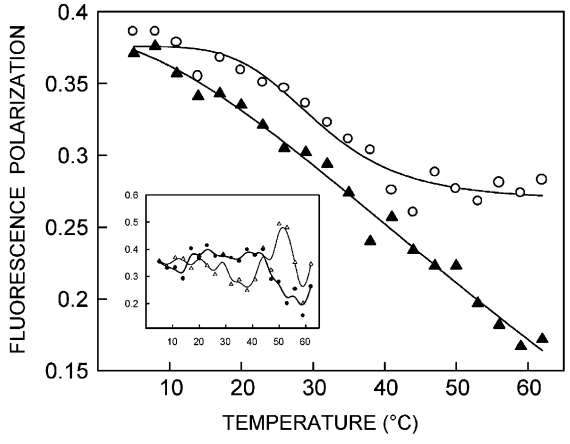

Fig. 8. Fluorescence polarization of DPH in liposomes of lipid extract from native membranes (○), and in liposomes of lipid extract from cholesterol-depleted (with 40 mM MβCD) membranes (▲) as a function of increasing temperature (5–62 °C). The inset shows fluorescence polarization of DPH in native membranes (△) and cholesterol-depleted (with 40 mM MβCD) membranes (●) as a function of increasing temperature. The excitation wavelength used was 358 nm and emission was monitored at 430 nm. The data were fitted with a sigmoidal regression analysis as described in Fig. 7. All other conditions are as in Fig. 3. See Materials and methods for other details.

long hydrophobic lauric acid chain [59]. Laurdan is also believed to show no preferential phase partitioning between ordered and disordered lipid phases and is considered to have uniform lateral and transbilayer distribution [60]. In addition, it has low affinity for proteins in the membrane [18]. These characteristics contribute in making Laurdan a well represented reporter molecule to sense molecular relaxation dynamics of solvent dipoles in the membrane as a whole.

Our results show that the emission spectra of Laurdan exhibit an additional red shifted peak as a function of increasing temperature in native as well as cholesterol-depleted membranes and liposomes made from lipid extracts of the native membrane. In addition, wavelength dependence of Laurdan GP in native membranes suggests the presence of ordered gel-like phase at low temperatures. Moreover, results from fluorescence polarization of DPH (Fig. 8) indicate that the hippocampal membrane is fairly ordered even at physiological temperature. The relevance of such ordered membrane in the context of the membrane function deserves comment. We have previously shown that although ordered, native hippocampal membranes provide appropriate environment and dynamics for the ligand binding function [25] and G-protein coupling ability [61] of the serotonin$_{1A}$ receptor. This is consistent with the emerging notion that in order for membrane to be functional, local rather than global fluidity plays a crucial role. Interestingly, we have recently shown that while oxidation of membrane cholesterol does not significantly perturb the overall membrane order as measured by fluorescence polarization of DPH, it results in a marked reduction in the serotonin$_{1A}$ receptor ligand binding function [62]. This points out to the lack of a direct correlation between membrane order and function.

Interestingly, we observe characteristics of liquid-ordered phase at high temperatures. Similar experiments performed using cholesterol-depleted membranes show fluidization of the membrane with increasing cholesterol depletion. It is apparent from (Figs. 3, 4, and 6) that while the phase state of the hippocampal membrane is sensitive to its cholesterol content, it is relatively insensitive to presence of proteins, especially at high temperatures. This is consistent with the known effect of cholesterol on the liquid-ordered phase in case of model membranes [50]. Importantly, the temperature dependence of Laurdan excitation GP provides additional information on the apparent thermal transition temperature and extent of cooperativity in these membranes. Mean fluorescence lifetime of Laurdan shows reduction with increase in temperature due to change in environmental polarity.

Taken together, our results constitute one of the first reports on dynamics of hippocampal membranes and its modulation by cholesterol depletion using Laurdan fluorescence. Our future efforts will focus on the relationship of these changes in dynamics with function of the hippocampal 5-HT$_{1A}$ receptor.

Acknowledgements

This work was supported by the Council of Scientific and Industrial Research, Government of India. A.C. is an honorary faculty member of the Jawaharlal Nehru Centre for Advanced Scientific Research, Bangalore (India). S.M. thanks the Council of Scientific and Industrial Research for the award of a Senior Research Fellowship. We gratefully acknowledge Md. Jafurulla, Sandeep Shrivastava and Thomas J. Pucadyil for help with the preparation of native membranes and cholesterol depletion from native membranes. Special thanks are due to Thomas J. Pucadyil, H. Raghuraman, and Md. Jafurulla for helpful discussions. We thank S. Rajanna for help with the tissue collection and members of our laboratory for critically reading the manuscript. We gratefully acknowledge Ganesh Bagler for his help with Fig. 1.

References

[1] P.S. Sastry, Lipids of nervous tissue: composition and metabolism, Prog. Lipid Res. 24 (1985) 69–176.
[2] K. Burger, G. Gimpl, F. Fahrenholz, Regulation of receptor function by cholesterol, Cell. Mol. Life Sci. 57 (2000) 1577–1592.
[3] T.J. Pucadyil, A. Chattopadhyay, Cholesterol modulates ligand binding and G-protein coupling to serotonin$_{1A}$ receptors from bovine hippocampus, Biochim. Biophys. Acta 1663 (2004) 188–200.
[4] G.I. Papakostas, D. Öngür, D.V. Iosifescu, D. Mischoulon, M. Fava, Cholesterol in mood and anxiety disorders: review of the literature and new hypotheses, Eur. Neuropsychopharmacol. 14 (2004) 135–142.
[5] J.M. Dietschy, S.D. Turley, Cholesterol metabolism in the brain, Curr. Opin. Lipidol. 12 (2001) 105–112.
[6] W.G. Wood, F. Schroeder, N.A. Avdulov, S.V. Chochina, U. Igbavboa, Recent advances in brain cholesterol dynamics: transport, domains, and Alzheimer's disease, Lipids 34 (1999) 225–234.
[7] J.J. Kabara, A critical review of brain cholesterol metabolism, Prog. Brain Res. 40 (1973) 363–382.
[8] S.D. Turley, D.K. Bruns, J.M. Dietschy, Preferential utilization of newly synthesized cholesterol for brain growth in neonatal lambs, Am. J. Physiol. 274 (1998) E1099–E1105.
[9] F.D. Porter, Malformation syndromes due to inborn errors of cholesterol synthesis, J. Clin. Invest. 110 (2002) 715–724.
[10] H.R. Waterham, R.J.A. Wanders, Biochemical and genetic aspects of 7-dehydrocholesterol reductase and Smith–Lemli–Opitz syndrome, Biochim. Biophys. Acta 1529 (2000) 340–356.
[11] T.J. Pucadyil, S. Kalipatnapu, A. Chattopadhyay, The serotonin$_{1A}$ receptor: a representative member of the serotonin receptor family, Cell. Mol. Neurobiol. (in press).
[12] A. Chattopadhyay, K.G. Harikumar, S. Kalipatnapu, Solubilization of high affinity G-protein-coupled serotonin$_{1A}$ receptors from bovine hippocampus using pre-micellar CHAPS at low concentration, Mol. Membr. Biol. 19 (2002) 211–220.
[13] T.J. Pucadyil, S. Shrivastava, A. Chattopadhyay, The sterol-binding antibiotic nystatin differentially modulates ligand binding of the bovine hippocampal serotonin$_{1A}$ receptor, Biochem. Biophys. Res. Commun. 330 (2004) 557–562.
[14] A. Chattopadhyay, Md. Jafurulla, S. Kalipatnapu, T.J. Pucadyil, K.G. Harikumar, Role of cholesterol in ligand binding and G-protein coupling of serotonin$_{1A}$ receptors solubilized from bovine hippocampus, Biochem. Biophys. Res. Commun. 327 (2005) 1036–1041.

[15] Y.D. Paila, T.J. Pucadyil, A. Chattopadhyay, The cholesterol-complexing agent digitonin modulates ligand binding of the bovine hippocampal serotonin$_{1A}$ receptor, Mol. Membr. Biol. 22 (2005) 241–249.
[16] T. Parasassi, G. De Stasio, A. d'Ubaldo, E. Gratton, Phase fluctuation in phospholipid membranes revealed by Laurdan fluorescence, Biophys. J. 57 (1990) 1179–1186.
[17] T. Parasassi, G. De Stasio, G. Ravagnan, R.M. Rusch, E. Gratton, Quantitation of lipid phases in phospholipid vesicles by the generalized polarization of Laurdan fluorescence, Biophys. J. 60 (1991) 179–189.
[18] T. Parasassi, E. Gratton, Membrane lipid domains and dynamics detected by Laurdan, J. Fluoresc. 5 (1995) 59–70.
[19] T. Parasassi, M. Di Stefano, M. Loiero, G. Ravagnan, E. Gratton, Influence of cholesterol on phospholipid bilayers phase domains as detected by Laurdan fluorescence, Biophys. J. 66 (1994) 120–132.
[20] K. Gaus, E. Gratton, E.P.W. Kable, A.S. Jones, I. Gelissen, L. Kritharides, W. Jessup, Visualizing lipid structure and raft domains in living cells with two-photon microscopy, Proc. Natl. Acad. Sci. U. S. A. 100 (2003) 15554–15559.
[21] R.P. Haugland, Handbook of Fluorescent Probes and Research Chemicals, 6th ed., Molecular Probes Inc., Eugene, OR, 1996.
[22] M. Murthy, J. Hamilton, R.S. Greiner, T. Moriguchi, N. Salem, H.-Y. Kim, Differential effects of n-3 fatty acid deficiency on phospholipid molecular species composition in the rat hippocampus, J. Lipid Res. 43 (2002) 611–617.
[23] L. Ulmann, V. Mimouni, S. Roux, R. Porsolt, J.-P. Poisson, Brain and hippocampus fatty acid composition in phospholipid classes of aged-relative cognitive deficit rats, Prostaglandins, Leukot. Essent. Fat. Acids 64 (2001) 189–195.
[24] Z. Wen, H.-Y. Kim, Alterations in hippocampal phospholipid profile by prenatal exposure to ethanol, J. Neurochem. 89 (2004) 1368–1377.
[25] K.G. Harikumar, A. Chattopadhyay, Metal ion and guanine nucleotide modulations of agonist interaction in G-protein-coupled serotonin$_{1A}$ receptors from bovine hippocampus, Cell. Mol. Neurobiol. 18 (1998) 535–553.
[26] P.K. Smith, R.I. Krohn, G.T. Hermanson, A.K. Mallia, F.H. Gartner, M.D. Provenzano, E.K. Fujimoto, N.M. Goeke, B.J. Olson, D.C. Klenk, Measurement of protein using bicinchoninic acid, Anal. Biochem. 150 (1985) 76–85.
[27] T.J. Pucadyil, A. Chattopadhyay, Exploring detergent insolubility in bovine hippocampal membranes: a critical assessment of the requirement for cholesterol, Biochim. Biophys. Acta 1661 (2004) 9–17.
[28] R.B. Gennis, Biomembranes: Molecular Structure and Function, Springer-Verlag, New York, 1989.
[29] D.M. Amundson, M. Zhou, Fluorometric method for the enzymatic determination of cholesterol, J. Biochem. Biophys. Methods 38 (1999) 43–52.
[30] E.G. Bligh, W.J. Dyer, A rapid method of total lipid extraction and purification, Can. J. Biochem. Physiol. 37 (1959) 911–917.
[31] C.W.F. McClare, An accurate and convenient organic phosphorus assay, Anal. Biochem. 39 (1971) 527–530.
[32] R. Koynova, M. Caffrey, Phases and phase transitions of the sphingolipids, Biochim. Biophys. Acta 1255 (1995) 213–236.
[33] D.E. Gueffroy (Ed.), Buffers: A Guide for The Preparation and Use of Buffers in Biological Systems, Calbiochem-Behring, San Diego, CA, 1983, p. 16.
[34] P.R. Bevington, Data Reduction and Error Analysis for the Physical Sciences, McGraw-Hill, New York, 1969.
[35] D.V. O'Connor, D. Phillips, Time-Correlated Single Photon Counting, Academic Press, London, 1984, pp. 180–189.
[36] R.A. Lampert, L.A. Chewter, D. Phillips, D.V. O'Connor, A.J. Roberts, S.R. Meech, Standards for nanosecond fluorescence decay time measurements, Anal. Chem. 55 (1983) 68–73.
[37] A. Grinvald, I.Z. Steinberg, On the analysis of fluorescence decay kinetics by the method of least-squares, Anal. Biochem. 59 (1974) 583–598.
[38] J.R. Lakowicz, Principles of Fluorescence Spectroscopy, Kluwer-Plenum Press, New York, 1999.
[39] A. Chattopadhyay, E. London, Fluorimetric determination of critical micelle concentration avoiding interference from detergent charge, Anal. Biochem. 139 (1984) 408–412.
[40] B.R. Lentz, B.M. Moore, D.A. Barrow, Light-scattering effects in the measurement of membrane microviscosity with diphenylhexatriene, Biophys. J. 25 (1979) 489–494.
[41] A.E. Christian, M.P. Haynes, M.C. Phillips, G.H. Rothblat, Use of cyclodextrins for manipulating cellular cholesterol content, J. Lipid Res. 38 (1997) 2264–2272.
[42] T. Parasassi, E.K. Krasnowska, L.A. Bagatolli, E. Gratton, Laurdan and Prodan as polarity sensitive fluorescence membrane probes, J. Fluoresc. 8 (1998) 365–373.
[43] S.S. Antollini, M.A. Soto, I.B. de Romanelli, C. Gutiérrez-Merino, P. Sotomayor, F.J. Barrantes, Physical state of bulk and protein-associated lipid in nicotinic acetylcholine receptor-rich membrane studied by Laurdan generalized polarization and fluorescence energy transfer, Biophys. J. 70 (1996) 1275–1284.
[44] L.A. Bagatolli, T. Parasassi, G.D. Fidelio, E. Gratton, A model for the interaction of 6-lauroyl-2-(*N,N*-dimethylamino)naphthalene with lipid environments: implications for spectral properties, Photochem. Photobiol. 70 (1999) 557–564.
[45] S. Mukherjee, A. Chattopadhyay, Wavelength-selective fluorescence as a novel tool to study organization and dynamics in complex biological systems, J. Fluoresc. 5 (1995) 237–246.
[46] A. Balter, W. Nowak, W. Pawelkiewicz, A. Kowalczyk, Some remarks on the interpretation of the spectral properties of Prodan, Chem. Phys. Lett. 143 (1988) 565–570.
[47] A. Samanta, R.W. Fessenden, Excited state dipole moment of PRODAN as determined from transient dielectric loss measurements, J. Phys. Chem., A 104 (2000) 8972–8975.
[48] L.P. Zanello, E. Aztiria, S. Antollini, F.J. Barrantes, Nicotinic acetylcholine receptor channels are influenced by the physical state of their membrane environment, Biophys. J. 70 (1996) 2155–2164.
[49] T. Parasassi, M. Loiero, M. Raimondi, G. Ravagnan, E. Gratton, Absence of lipid gel-phase domains in seven mammalian cell lines and in four primary cell types, Biochim. Biophys. Acta 1153 (1993) 143–154.
[50] D.A. Brown, E. London, Structure and origin of ordered lipid domains in biological membranes, J. Membr. Biol. 164 (1998) 103–114.
[51] S. Palleschi, L. Silvestroni, Laurdan fluorescence spectroscopy reveals a single liquid-crystalline lipid phase and lack of thermotropic phase transitions in the plasma membrane of living human sperm, Biochim. Biophys. Acta 1279 (1996) 197–202.
[52] J.B. Massey, Interaction of ceramides with phosphatidylcholine, sphingomyelin and sphingomyelin/cholesterol bilayers, Biochim. Biophys. Acta 1510 (2001) 167–184.
[53] F.G. Prendergast, Time-resolved fluorescence techniques: methods and applications in biology, Curr. Opin. Struct. Biol. 1 (1991) 1054–1059.
[54] T. Parasassi, M. Di Stefano, M. Loiero, G. Ravagnan, E. Gratton, Cholesterol modifies water concentration and dynamics in phospholipid bilayers: a fluorescence study using Laurdan probe, Biophys. J. 66 (1994) 763–768.
[55] B.R. Lentz, Membrane fluidity as detected by diphenylhexatriene probes, Chem. Phys. Lipids 50 (1989) 171–190.
[56] W. Yu, P.T.C. So, T. French, E. Gratton, Fluorescence generalized polarization of cell membranes: a two-photon scanning microscopy approach, Biophys. J. 70 (1996) 626–636.
[57] S.S. Antollini, F.J. Barrantes, Disclosure of discrete sites for phospholipid and sterols at the protein–lipid interface in native acetylcholine receptor-rich membrane, Biochemistry 37 (1998) 16653–16662.
[58] A. Chattopadhyay, E. London, Parallax method for direct measurement of membrane penetration depth utilizing fluorescence quenching by spin-labeled phospholipids, Biochemistry 26 (1987) 39–45.

[59] J. Zeng, P.L. Chong, Effect of ethanol-induced lipid interdigitation on the membrane solubility of Prodan, Acdan, and Laurdan, Biophys. J. 68 (1995) 567–573.
[60] L.A. Bagatolli, E. Gratton, Direct observation of lipid domains in free-standing bilayers using two-photon excitation fluorescence microscopy, J. Fluoresc. 11 (2001) 141–160.
[61] K.G. Harikumar, A. Chattopadhyay, Differential discrimination of G-protein coupling of serotonin$_{1A}$ receptors from bovine hippocampus by an agonist and an antagonist, FEBS Lett. 457 (1999) 389–392.
[62] T.J. Pucadyil, S. Shrivastava, A. Chattopadhyay, Membrane cholesterol oxidation inhibits ligand binding function of hippocampal serotonin$_{1A}$ receptors, Biochem. Biophys. Res. Commun. 331 (2005) 422–427.